

the full resonance energy of naphthalene (61 kcal/mol) to the transition state".

The intrinsic activation energy for the $[\pi_{2s} + \sigma_{2s} + \sigma_{2s}]$ concerted dihydrogen exchange appears to be very high and one is left to wonder whether there may exist a nonconcerted pathway with a lower activation energy.

The reaction discussed here is not the only case where a Woodward-Hoffman-allowed reaction has in fact a high activation energy. For instance, Feller et al.²² have recently found calculated barriers of 30 and 50 kcal/mol for two other "allowed" concerted

pericyclic shifts of three reactive electron pairs, namely, the decompositions of dihydroxycarbene and 2-carbena-1,3-dioxolane.

Acknowledgment. We wish to express our thanks to Dr. Stephen Elbert, whose constant improvements to the ALIS program system made these calculations feasible. We also extend our thanks to Professor Richard P. Johnson for a critical reading of the manuscript and very valuable comments. The vibrational analysis calculations were performed on the Chemistry Department VAX computer at the University of Washington. The present work was supported by the U.S. Department of Energy, Director of Energy Research, Office of Basic Energy Science, under Contract No. W-7405-Eng-82.

(22) Feller, D.; Borden, W. T.; Davidson, E. R. *J. Comput. Chem.* **1980**, *1*, 158-166. Feller, D.; Davidson, E. R.; Borden, W. T. *J. Am. Chem. Soc.* **1981**, *103*, 2558-2560.

Registry No. Ethane, 74-84-0; ethylene, 74-85-1.

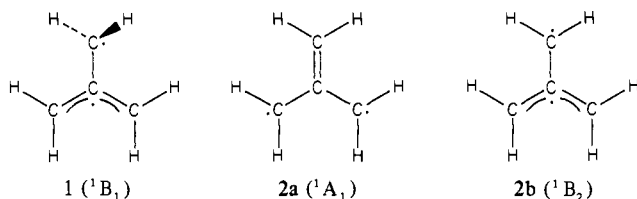
Potential Surface for the Methylene-cyclopropane Rearrangement

David Feller, Kiyoshi Tanaka, Ernest R. Davidson,* and Weston Thatcher Borden*

Contribution from the Department of Chemistry, University of Washington, Seattle, Washington 98195. Received August 13, 1981

Abstract: MCSCF calculations with an STO-3G basis set have been carried out to obtain the optimal geometries and associated energies for a grid of points on the lowest singlet potential surface connecting methylenecyclopropane (MCP) and trimethylenemethane (TMM). Two methylene rotation angles were used to generate a two-dimensional projection of the 24-dimensional hypersurface, and a double Fourier fit to the computed energies gave a closed form expression for the energy on the two-dimensional surface. Three minima, connected by four transition states, were located on the surface. The effect of basis set expansion and inclusion of CI on the relative energies was determined. In accord with Hammond's postulate, the energies of transition states leading to orthogonal and planar TMM were found to be in the same order as the energies of these two intermediates. The conrotatory transition state leading to planar TMM was found to be slightly lower in energy than the disrotatory one. From a Fourier fit to the triplet energies, calculated at the optimal singlet geometries on the two-dimensional surface, the line along which the singlet and triplet surfaces intersect has been found. The lowest point along this line was computed to be higher in energy than orthogonal TMM. The implications of this finding are discussed.

The thermal rearrangements of methylenecyclopropane (MCP) derivatives have been the subject of numerous experimental investigations.¹ These studies suggest that the major pathway involves the orthogonal geometry (**1**) in which one methylene group



is twisted 90° out of conjugation with the rest of the π system.²⁻⁷ However, a small amount of planar (**2**) trimethylenemethane (TMM) is apparently also formed.⁸⁻¹⁰

The preference for **1** over **2** in the lowest singlet state contrasts with the geometry of the lowest triplet state. Both the null value of the zero field splitting parameter E^{11} and the hyperfine coupling pattern¹² suggest a triplet geometry of at least C_3 symmetry. Ab initio calculations predict the triplet geometry to be planar D_{3h} .¹³ The difference between the preferred geometry of the singlet and triplet has been rationalized in terms of electron repulsion effects.¹⁴

A large number of calculations have been carried out to determine the relative energies of the planar and orthogonal singlet states, and all predict that the orthogonal singlet is lower.¹⁵⁻²³

(1) Gajewski, J. J. "Hydrocarbon Thermal Isomerizations"; Academic Press: New York, 1981.

(2) Ullman, E. F. *J. Am. Chem. Soc.* **1960**, *82*, 505.

(3) Gajewski, J. J. *J. Am. Chem. Soc.* **1971**, *93*, 4450.

(4) Doering, W. von E.; Roth, H. D. *Tetrahedron* **1970**, *26*, 2825.

(5) Doering, W. von E.; Birladeanu, L. *Tetrahedron* **1973**, *29*, 449.

(6) Gilbert, J. C.; Butler, J. R. *J. Am. Chem. Soc.* **1970**, *92*, 449.

(7) Jones, M.; Hendrick, M. E.; Gilbert, J. C.; Butler, J. R. *Tetrahedron Lett.* **1970**, 845.

(8) Buchwalter, S. G. Ph.D. Thesis, Harvard 1974; *Diss. Abstr. Int. B* **1974**, *35*, 1564.

(9) Roth, W.; Wegener, G. *Angew. Chem., Int. Ed. Engl.* **1975**, *14*, 758.

(10) Gajewski, J. J.; Chou, S. K. *J. Am. Chem. Soc.* **1977**, *99*, 5696.

(11) Dowd, P. *J. Am. Chem. Soc.* **1966**, *88*, 2587.

(12) Dowd, P.; Gold, A.; Sachdev, K. *J. Am. Chem. Soc.* **1968**, *90*, 2715.

(13) Hood, D. M.; Pitzer, R. M.; Schaefer, H. F.; III *J. Am. Chem. Soc.* **1978**, *100*, 2227.

(14) Borden, W. T.; Salem, L. *J. Am. Chem. Soc.* **1973**, *95*, 932.

(15) Dewar, M. J. S.; Wasson, J. S. *J. Am. Chem. Soc.* **1971**, *93*, 3081.

(16) Hehre, W. J.; Salem, L.; Willcott, M. R. *J. Am. Chem. Soc.* **1974**, *96*, 4328.

(17) Yarkony, D. R.; Schaefer, H. F., III *J. Am. Chem. Soc.* **1974**, *96*, 3754.

(18) Davidson, E. R.; Borden, W. T. *J. Chem. Phys.* **1976**, *64*, 663.

However, two of these calculations^{15,16} predict an erroneously large energy difference because of their failure to obtain correct wave functions for the planar singlet.^{24,25}

There are, in fact, two planar singlet states, represented by **2a** and **2b**. Their wave functions in C_{2v} symmetry are respectively 1A_1 and 1B_2 , which become the two degenerate components of the $^1E'$ state at D_{3h} geometries. Second-order Jahn–Teller effects cause the energy of 1A_1 (**2a**) at its equilibrium geometry to lie below that of 1B_2 (**2b**) on the lowest singlet potential surface for the unsubstituted molecule.^{20,23} The relevant comparison for the energy difference between the orthogonal and planar geometries is therefore between 1B_1 (**1**) and 1A_1 (**2a**).

If both **1** and **2a** are intermediates, kinetic experiments cannot provide the energy difference between them but only between the transition states leading to them. From Hammond's postulate²⁶ one would anticipate that the relative energies of the transition states should parallel those of the diradical intermediates. One goal of the theoretical study reported in this paper was to determine whether this was, in fact, the case.

Two previous studies have calculated the transition state connecting MCP and **1**.^{16,22} However, calculations along the pathway connecting MCP and **2a** have not been reported. Consequently, it is not known whether there is any preference for a conrotatory or disrotatory transition state, much less what the energy of the lower of these two is, relative to that of the transition state leading to **1**. Indeed, it has not even been established whether **2a** is a true intermediate on the lowest singlet surface.

The relative energies of the lowest singlet and triplet surfaces at various geometries also remain to be established. Only the energy difference between 1B_1 and of $^3A'_2$ TMM has been computed previously.^{16–23,27} The triplet is found to be between 14 and 21 kcal/mol below the singlet, with the best calculations giving the smallest energy difference.²⁷

Dowd has measured the temperature dependence of the rate of disappearance of the EPR signal in triplet TMM.²⁸ Depending on how the triplet TMM was generated, energies of activation between 2.0 and 7.8 kcal/mol were obtained. If the energy difference between 1B_1 and $^3A'_2$ is being measured by these experiments, this difference, even at the upper end of the range, is only about half of that computed by the best ab initio calculations.

It has been pointed out, however, that if the disappearance of the EPR signal is due to closure to MCP by crossing of the triplet to the single surface, the lowest surface intersection could occur at energies below that of 1B_1 .²⁹ This suggestion, if correct, could reconcile the theoretically calculated energy gap between 1B_1 and $^3A'_2$ with Dowd's experimental results. Testing this hypothesis, which requires determining the lowest energy at which the surface crossing occurs, was one of the chief goals of this study.

At planar geometries, the triplet is computed to lie roughly 20 kcal/mol below the singlet. In contrast, at the geometry of MCP, the global minimum on the singlet surface, the lowest triplet is very high in energy, compared to the singlet. With this gross description of the relative energies of the two surfaces as a function of the methylene rotation angles, the only hope for discovering a low-energy surface crossing in the general vicinity of the planar triplet is to observe a rapid descent in energy of the singlet surface in directions leading from TMM to MCP. Thus, we began by finding optimal singlet geometries for various methylene rotation angles.

Methodology

Because the principal differences in geometry among all previously known conformations of interest on the singlet MCP–TMM surface involved rotation of one or two methylene groups about the C(methylene)–C(central) bonds, we decided to study a projection of the full 24-dimensional energy hypersurface onto the methylene rotational plane. The two rotation angles, ϕ_1 and ϕ_2 , that serve as the coordinates for this projection are defined as the dihedral angles X–C(methylene)–C(central)–C(methylene), where X is a point along a line that is perpendicular to the HCH plane of each methylene group and that intersects the plane at C(methylene). The bond angle X–C(methylene)–C(central) may be taken as a measure of the extent of pyramidalization at the methylene site, with 90° representing no pyramidalization. Apart from ϕ_1 and ϕ_2 , all 22 other internal coordinates are optimal in this projection.

A Dunning split valence (SV) contraction, (3s,2p/2s),³⁰ of the Huzinaga [9s,5p/4s] primitive basis³¹ was chosen for our CI calculations. However, given the very large number of calculations required for geometry optimizations over a large potential surface, the 3-21G³² basis, which contains the same number of contracted orbitals but fewer gaussian primitives, was first tested as a computationally economical substitute. Agreement was good between the geometries for $^3A'_2$ and 1B_1 TMM that were calculated with this basis set and those reported by Hood, Schaefer, and Pitzer²⁷ with the Dunning double ζ (DZ) basis.³³ Carbon–carbon bond lengths were shorter by about 0.01 Å with the smaller basis set. The minimal STO-3G³⁴ basis set actually produced results slightly closer to the DZ basis than did 3-21G. Both of the smaller basis sets gave reasonable agreement between the structure computed for MCP and that obtained by microwave spectroscopy.³⁵ Since the 3-21G basis appeared to offer no clear cut advantage for the initial geometry optimization, it was abandoned in favor of the STO-3G basis.

Exploratory two-configuration self-consistent field (TCSCF) calculations were performed along the conrotatory and disrotatory paths connecting 1A_1 TMM and MCP. Two configurations are the minimal number needed to describe the bond-breaking process leading to a diradical. The results suggested the existence of low barriers, on the order of 2–4 kcal/mol, for closure of 1A_1 TMM to MCP.

However, in order to provide a complete description of the global singlet potential surface, it was desirable to compute a grid in (ϕ_1 , ϕ_2). Unfortunately, the so-called "doublet instability" phenomenon³⁶ would have rendered any spin restricted Hartree–Fock (RHF) results useless in the vicinity of the 1B_1 ($\phi_1 = 90$, $\phi_2 = 0$) point.³⁷ This instability is characterized by the tendency of RHF wave functions for radicals and diradicals to localize the unpaired electrons. The problem is worst when minimal basis sets are employed, and it can lead to broken symmetry solutions of the RHF equations at symmetric geometries.

A well-studied example of this effect occurs in the allyl radical.³⁶ Since the 1B_1 TMM wave function contains an allyl radical fragment, a wave function of broken symmetry would be anticipated, unless C_{2v} symmetry were imposed on it. Although it would have been possible to obtain a C_{2v} constrained 1B_1 RHF wave function at the orthogonal geometry, the energy of this wave function and the relative energies and geometries near (90, 0) would have been skewed by the doublet instability effect.

Therefore, a full multiconfiguration SCF (MCSCF) wave function in the orbital space of the four out-of-plane carbon p

(19) Davis, J. H.; Goddard, W. A. *J. Am. Chem. Soc.* **1976**, *98*, 303.

(20) Davidson, E. R.; Borden, W. T. *J. Am. Chem. Soc.* **1977**, *99*, 2053.

(21) Davis, J. H.; Goddard, W. A. *J. Am. Chem. Soc.* **1977**, *99*, 4242.

(22) Dixon, D. A.; Foster, R.; Halgren, T. A.; Lipscomb, W. N. *J. Am. Chem. Soc.* **1978**, *100*, 1359.

(23) Dixon, D. A.; Dunning, T. H., Jr.; Eades, R. A.; Kleier, D. A. *J. Am. Chem. Soc.* **1981**, *103*, 2878.

(24) Borden, W. T. *J. Am. Chem. Soc.* **1975**, *97*, 2906.

(25) Borden, W. T. *J. Am. Chem. Soc.* **1976**, *98*, 2695.

(26) Hammond, G. S. *J. Am. Chem. Soc.* **1955**, *77*, 334.

(27) Hood, D. M.; Schaefer, H. F., III; Pitzer, R. M. *J. Am. Chem. Soc.* **1979**, *100*, 8009.

(28) Dowd, P.; Chow, M. *J. Am. Chem. Soc.* **1977**, *99*, 6438.

(29) Borden, W. T.; Davidson, E. R. *Annu. Rev. Phys. Chem.* **1979**, *30*, 125.

(30) Dunning, T. H., Jr.; Hay, P. J. In "Modern Theoretical Chemistry"; Vol. 2, ed. Schaefer, H. F., III Ed.; Plenum Press: New York, 1977; Vol. 2.

(31) Huzinaga, S. *J. Chem. Phys.* **1965**, *42*, 1293.

(32) Binkley, J. S.; Pople, J. A.; Hehre, W. J. *J. Am. Chem. Soc.* **1980**,

102, 939.

(33) Dunning, T. H., Jr. *J. Chem. Phys.* **1970**, *53*, 2823.

(34) Hehre, W. J.; Stewart, R. F.; Pople, J. A. *J. Chem. Phys.* **1969**, *51*,

2657.

(35) Laurie, V. W.; Stigliani, W. M. *J. Am. Chem. Soc.* **1970**, *92*, 1485.

(36) Paulus, J.; Vellard, A. *Mol. Phys.* **1978**, *35*, 445 and references therein.

(37) Borden, W. R.; Davidson, E. R.; Feller, D. *Tetrahedron*, in press.

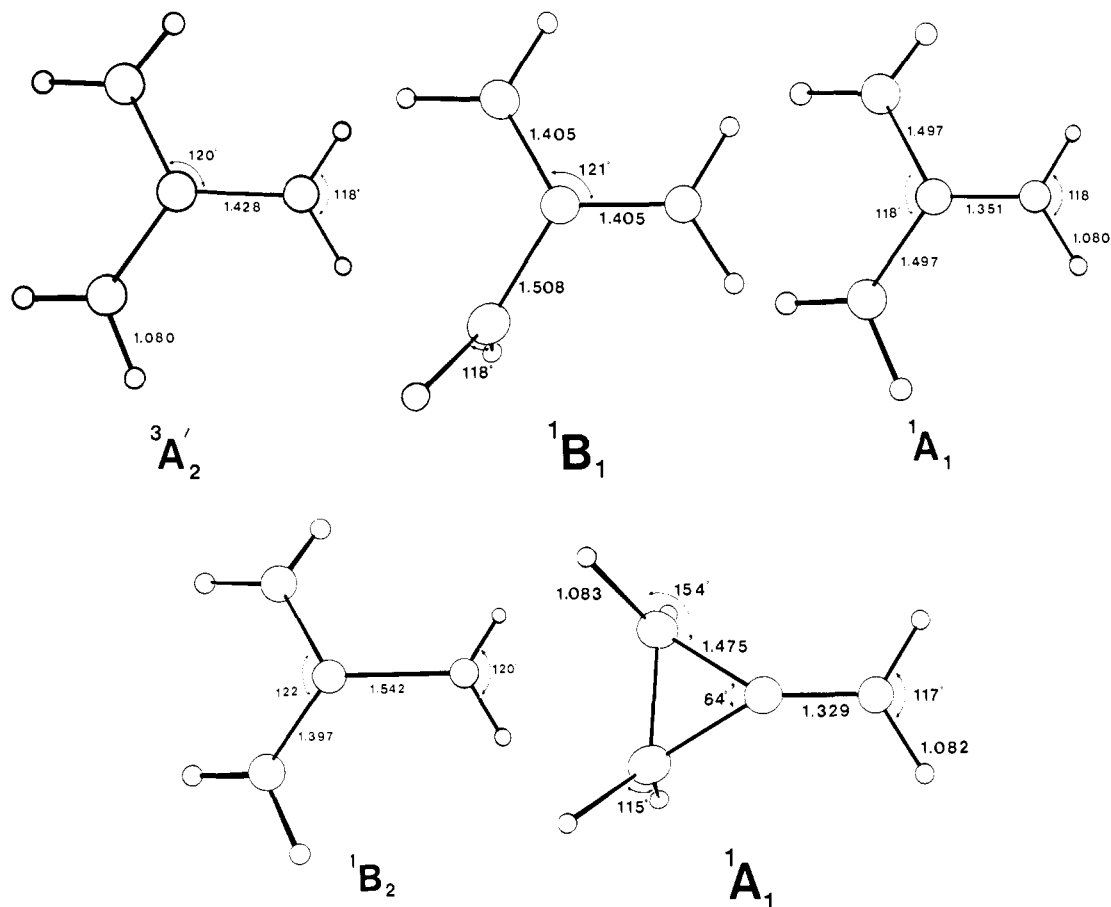


Figure 1. Optimal geometries for some stationary points on the singlet and triplet potential energy surfaces for the methylenecyclopropane rearrangement. Geometries were optimized with MCSCF calculations, using an STO-3G basis set.

Table I. Total Energies (Hartrees) at the Optimal STO-3G Geometries

	STO-3G			SV(3s,2p/2s)		SVP(3s,3p,1d/2s,1p) RHF/TCSCF ^b
	RHF/TCSCF ^a	MCSCF ^b	SDQ-CI ^{b,c}	RHF/TCSCF ^b	SDQ-CI ^{b,c}	
MCP ¹ A ₁	-153.0112	-153.0702	-153.293	-154.8219	-155.195	-154.9057
TMM ³ A ₂ '	-152.9698 (26.0) ^d	-153.0321 (23.9)	-153.247 (28.9)	-154.8149 (4.4)	-155.183 (7.5)	-154.8861 (12.3)
TMM ¹ B ₁	-152.9447 (41.7)	-153.0078 (39.2)	-153.223 (43.9)	-154.7908 (19.5)	-155.155 (25.1)	-154.8633 (26.6)
TMM ¹ A ₁	-152.9594 (32.5)	-152.9984 (45.1)	-153.214 (49.6)	-154.7980 (15.0)	-155.154 (25.7)	-154.8700 (22.4)
TMM ¹ B ₂	-152.9403 (44.5)	-152.9970 (45.9)	-153.213 (50.0)	-154.7874 (21.6)	-155.149 (28.9)	
TS 1 ^e	-152.9557 (34.8)	-152.9971 (45.9)		-154.7922 (18.6)	-155.157 (23.8)	
TS 1 ^e	-152.9566 (34.3)	-152.9965 (46.2)		-154.7918 (18.6)	-155.154 (25.7)	
TS 3 ^e	-152.9585 (33.1)	-152.9990 (44.7)		-154.7941 (17.5)	-155.158 (23.2)	

^a Geometries optimized with RHF or TCSCF wave functions. ^b Geometries optimized with (4-orbitals/4-electron) MCSCF wave function. ^c Single and double excitation CI with correction for quadruple excitations. ^d Energy in kcal/mol, relative to MCP at the same level of theory. ^e Transition state 1 connects ¹A₁, TMM and MCP along conrotary path. Transition state 2 connects ¹A₁, TMM and MCP along disrotary path. Transition state 3 connects ¹B₁, TMM and MCP.

orbitals was employed for the geometry optimizations. This wave function represents the minimal level of theory capable of providing a balanced description of the global singlet surface. Dixon et al.²³ have recently used such a wave function in their study of the electronic states of TMM and the related compound, 2-methylenecyclopentane-1,3-diyli. As they note, this full 4-orbital/4-electron MCSCF wave function is equivalent to a full π space CI for planar TMM. It has been shown computationally that full π space CI is sufficient for obtaining ¹A₁ and ¹B₂ wave functions that exhibit the correct degeneracy at D_{3h} geometries.¹⁸

Constrained internal coordinate geometry optimizations were performed with GAMESS,³⁸ an analytical gradient, MCSCF program from the National Resource for Computation in Chemistry. All other calculations were carried out by using programs written in this group.

Results

Optimal geometries obtained with the STO-3G basis at some of the stationary points on the singlet and triplet potential surfaces are shown in Figure 1. These geometries are in essential agreement with the RHF and TCSCF geometries of Dixon et al.,²³ obtained with the PRDDO integral approximation and a minimal Slater-type orbital (STO) basis and with our own symmetry constrained RHF and TCSCF calculations with the STO-3G basis. RHF, TCSCF and MCSCF energies at the optimal STO-3G geometries are given in Table I.

Over most of the lowest singlet surface the four TMM carbon atoms remained coplanar to within $\pm 3^\circ$. However, for the points near MCP, the molecule began to buckle out of plane in order to allow closer approach of the twisting methylene carbons and, thus, earlier ring formation. As this distortion greatly increased the time required for geometry optimization in a relatively uninteresting portion of the potential surface, it was decided to impose the additional constraint of planarity on the four carbons at these

(38) Dupuis, M.; Spangler, D.; Wendoloski, J. J. GAMESS, NRCC Software Catalog; 1980; Vol. 1, Prog. No. QG01.

points. The effect that this constraint has is to make the slope of the surface leading toward MCP gentler than it actually is in this region.

Another phenomenon that was observed was the tendency with the STO-3G basis for some of the methylene centers to pyramidalize. The magnitude of the effect was investigated at the 1A_1 , 1B_2 , and (135, 45) disrotary geometries. At the optimal 1A_1 point diagonalization of the hessian matrix of energy second derivatives showed two negative eigenvalues at both the TCSCF and MCSCF levels of theory. These normal modes, with imaginary frequencies $453i$ and $491i$ cm^{-1} , corresponded to pyramidalization of the two equivalent methylene groups in the same and in opposite directions. However, on switching to the 3-21G basis, the two negative eigenvalues changed sign, while remaining nearly constant in magnitude.

An STO-3G MCSCF geometry optimization was begun near planar 1A_1 but with the two equivalent methylenes slightly pyramidalized. The final geometry did show a significant degree of methylene group pyramidalization, with X-C(methylene)-C-(central) angles of 66° for the two equivalent methylenes, compared to 90° for no pyramidalization. Nevertheless, the energy was only 0.0011 hartrees (0.7 kcal/mol) below the C_{2v} constrained geometry. By way of comparison, in methane this angle is 35° .

When this procedure was repeated at a slightly distorted geometry near 1B_1 , essentially no pyramidalization was observed for the two allylic methylenes in the final optimal geometry. At the (135, 45) disrotary point, a difference in methylene pyramidalization of about 8° between STO-3G and 3-21G was noted for calculations at the TCSCF level of theory.

The extent to which the STO-3G basis gives pyramidalized methylene centers, which are not pyramidalized with larger basis sets, depends on the strength of the π bond associated with these centers. For instance, in 1B_1 the strong π bonds to the allylic methylenes makes pyramidalization of these carbons unfavorable, even with STO-3G. In contrast, the weaker π bonds to these carbons in 1A_1 allow the methylene groups to pyramidalize with STO-3G. Consequently, with this basis set, not only 1A_1 but also the optimal geometries along the conrotary and disrotary paths show a spurious tendency toward pyramidalization of the two equivalent methylene groups. Fortunately, however, the energetic consequences of this effect are slight. The energies in Table I were calculated by using the optimal C_{2v} geometry for 1A_1 in which the methylene groups are all planar.

Within the region of the potential surface bounded by $\phi_1, \phi_2 = 0^\circ$ and 180° , there are only 21 unique points on a grid with 22.5° intervals in these two angles. Consequently, it was practical to calculate the energies of these 21 points in order to fit them with a double Fourier series in the two rotation angles.³⁹ This gave a closed form expression for the energy on the singlet surface as a function of (ϕ_1, ϕ_2) with all 22 other geometrical parameters optimized.

A similar expression was obtained for the energy on the triplet surface as a function of (ϕ_1, ϕ_2) , but the triplet calculations were carried out at the optimized singlet geometries. Therefore, the triplet surface, whose energy is given by the Fourier series, does not correspond to a projection in which the other 22 geometric parameters are optimized.

Because of the cmm two-dimensional space group symmetry possessed by the surface,³⁹ only terms of the form

$$\begin{aligned} \cos(2k\phi_1)\cos(2l\phi_2) + \cos(2l\phi_1)\cos(2k\phi_2) & \quad k, l = 0-4 \\ \sin(2k\phi_1)\sin(2l\phi_2) + \sin(2l\phi_1)\sin(2k\phi_2) & \quad k, l = 1-3 \end{aligned}$$

can have nonzero coefficients. Values of the Fourier coefficients for both singlet and triplet surfaces are presented in Table II.

A contour map of the singlet surface (contour increment = 0.001 hartree) is shown in Figure 2. In contrast to the wealth of structure that is evident on this surface, the triplet surface, computed with the same geometries, shows only a minimum ($\phi_1 = 0, \phi_2 = 0$) and a maximum ($\phi_1 = 90, \phi_2 = 90$). The heavy

Table II. Fourier Expansion Coefficients for the STO-3G MCSCF Surfaces

	<i>k</i>	<i>l</i>	singlet	triplet
Sine Terms				
(1)	1	1	-0.000 182	-0.000 052
(2)	1	2	0.000 207	0.000 013
(3)	2	2	-0.000 175	0.000 000
(4)	1	3	-0.000 125	0.000 000
(5)	2	3	0.000 182	-0.000 013
(6)	3	3	-0.000 093	0.000 002
Cosine Terms				
(7)	1	1	-0.005 551	0.011 039
(8)	1	2	0.008 600	-0.009 113
(9)	2	2	-0.001 956	0.003 184
(10)	1	3	-0.000 138	0.000 031
(11)	2	3	0.001 175	-0.001 600
(12)	3	3	-0.000 937	0.001 917
(13)	1	4	-0.001 196	0.001 902
(14)	2	4	0.000 156	0.000 016
(15)	3	4	0.000 996	-0.001 908
(16)	4	4	-0.000 389	0.000 802
(17)	0	1	0.008 766	-0.020 507
(18)	0	2	-0.006 219	0.004 353
(19)	0	3	-0.000 391	-0.001 300
(20)	0	4	0.000 497	-0.001 602
(21)	0	0	-153.005 228	-152.997 333

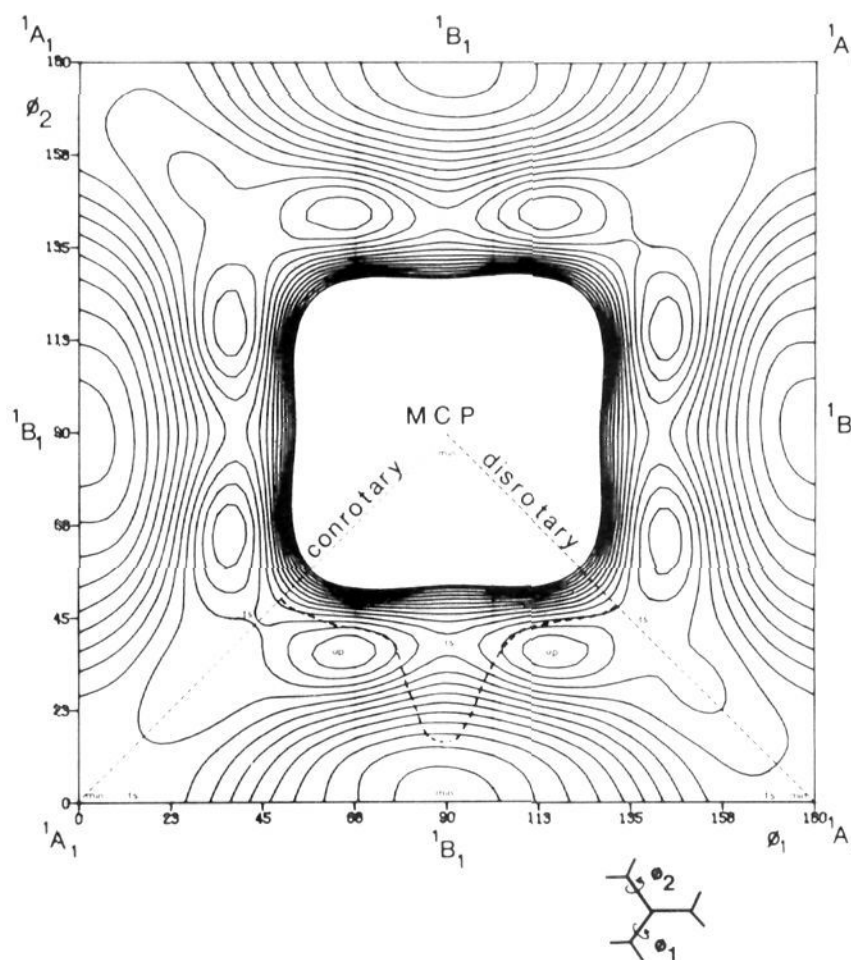


Figure 2. Contour map of the lowest singlet potential energy surface for the methylenecyclopropane rearrangement as a function of two methylene rotation angles with all other geometrical parameters optimized. Contour increments are 0.001 hartree. The heavy dashed line represents the intersection of the singlet and triplet surfaces when the energies of both are computed at the optimal singlet geometries.

dashed line, displayed in only one of the four identical quadrants, represents the line of intersection of the two surfaces. The lowest energy along the line occurs near $\phi_1 = 88^\circ$ and $\phi_2 = 15^\circ$.

The MCSCF energy at this point is -153.005 hartrees, almost 2 kcal/mol higher than that of 1B_1 . Thus, at least at the STO-3G MCSCF level of theory, there appears to be no crossing of the singlet and triplet surfaces below the energy of 1B_1 . The lowest energy surface crossing is, therefore, at least 15 kcal/mol above ${}^3A'_2$.

Four unique transition states in the triangular region of the contour map in Figure 2 are predicted by the Fourier fit to the singlet surface. Two of these connect 1A_1 TMM and MCP, one

(39) Feller, D.; Borden, W. T.; Davidson, E. R. *J. Chem. Phys.* **1979**, *71*, 4987.

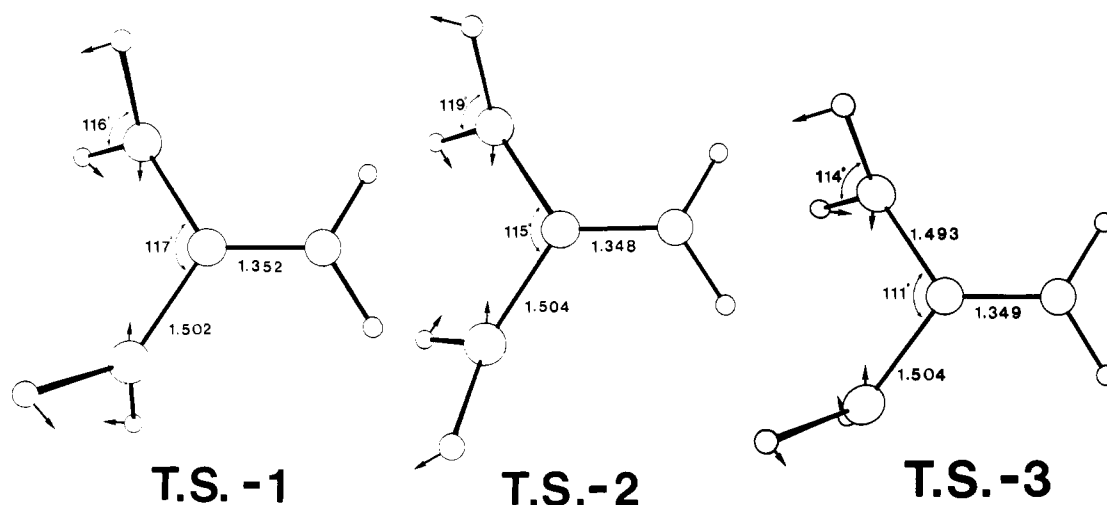


Figure 3. Three transition-state geometries on the lowest singlet potential energy surface for the methylenecyclopropane rearrangement. The arrows indicate the mass weighted reaction coordinates.

along the conrotary and the other along the disrotary path. The third connects 1B_1 TMM and MCP; and the fourth, which is invisible in the figure, due to insufficiently fine contour increments, connects the 1A_1 and 1B_1 minima.

Diagonalization of the mass-weighted hessian matrices each yielded one negative eigenvalue, confirming that the first three points were transition states. The geometries are shown in Figure 3, along with the reaction coordinates. The energies are given in Table I. The reaction coordinates have imaginary frequencies of 220i, 209i, and 261i cm^{-1} , respectively, indicating very flat regions of the potential surface in the proximity of these transition states. It was decided not to attempt to confirm the fourth transition state because of the complication from STO-3G pyramidalization of the methylenes at geometries near 1A_1 . The Fourier fit predicts that this last transition state is about 0.001 hartrees above the 1A_1 .

Dixon et al.²² have reported a PRDDO maximum along the linear synchronous transit path connecting 1B_1 and MCP. Hehre et al.¹⁶ also obtained an optimized structure at the maximum along a path connecting these two singlet minima. Both geometries are similar to that of our true transition state but differ from it in detail. Our STO-3G MCSCF activation energy of 44.7 kcal/mol is comparable to the values calculated by these two groups and to the experimental value of 40.4 kcal/mol for rearrangement of 2-methyl methylenecyclopropane.⁴⁰

Basis set enlargement greatly affects the computed relative stability of MCP with respect to the rest of the singlet surface. For instance, as seen in the data of Table I, the MCP-TMM ($^3A'_2$) RHF energy difference changes from 26.0 to 4.4 to 12.3 kcal/mol in going from STO-3G to Dunning SV to Dunning SV plus polarization (SVP) basis sets. All of these values were obtained at the optimal STO-3G geometries. With the SV basis, addition of polarization functions is necessary in order to describe properly the bonding in the strained, three-membered ring of MCP.⁴¹

The relative energies of other points on the potential surfaces are less affected by basis set expansion. The singlet-triplet gap, as measured by the difference in RHF energy between $^3A'_2$ and 1B_1 , appears insensitive to increases in basis set size, as has been previously noted by Hood, Pitzer, and Schaefer.²⁷ The SVP value of 14.3 kcal/mol is within 2 kcal/mol of the STO-3G and SV values.

Table I shows that recovery of a larger fraction of the valence correlation energy than is possible with the 4-orbital/4-electron MCSCF wave function has relatively little effect on the surface. Configuration interaction (CI) calculations which included all single and double excitations from an SCF/TCSCF reference wave function were performed with the STO-3G basis. A correction

was made to account for the effect of neglected quadruple excitations.⁴² With the SV basis the virtual orbitals were first transformed to K orbitals.⁴³ These orbitals have been shown to closely approximate the frozen natural orbitals of many low-lying molecular states. Second-order perturbation theory was then used to select the energetically most important configurations from among the full set. For example, of the approximately 39 000 spin-adapted configurations generated by single and double excitations with respect to the TCSCF 1A_1 reference wave function, only some 3600 were kept. The perturbation estimate of the amount of energy associated with the configurations thrown away was scaled by the ratio of the actual CI energy lowering and the perturbation estimate of this quantity. Some 80% of the SD correlation energy was variationally recovered. Past experience has shown that when the CI recovers about 80% of the SD energy, the scaling estimate of the energy thrown away is accurate to $\pm 2\%$, a few millihartrees in this case.

The final SV SDQ-CI value for the $^3A'_2 - ^1B_1$ energy gap is 17.6 kcal/mol. The energies at the conrotary, disrotary, and asymmetric STO-3G MCSCF transition state geometries are in the same order as they were with the STO-3G MCSCF wave functions. However, the purported disrotary transition state is now equal in energy to 1A_1 TMM, and the conrotary is slightly below it. The purported transition state leading to 1B_1 is also slightly below 1B_1 in energy.

Discussion

It seems likely that the transition states, found with the STO-3G basis set, shift on expansion of the basis set to SV. Hammond's postulate²⁶ would predict that a change in the positions of the transition state should accompany the 15–20-kcal/mol change in the computed energy of MCP relative to TMM. Further changes in the positions of the transition states probably occur on expansion of the basis set from SV to SVP.

The true effect of basis set enlargement on relative energies can only be accurately measured with geometries that are optimal for each set. As shown by the results in Table I, geometry optimization for each basis set appears to be particularly important for transition states that occur in relatively flat regions on potential surfaces. Unfortunately, using an SVP basis set and an MCSCF wave function to optimize completely the geometries for a molecule the size of TMM is prohibitively expensive.

Despite the uncertainties associated with carrying out calculations with large basis sets at geometries optimized with small ones, the relative SV and SVP energies in the TMM portion of the surface are in qualitative agreement with the comparable STO-3G results. It seems reasonable to believe, therefore, that

(40) Chesick, J. P. *J. Am. Chem. Soc.* **1963**, *85*, 2720.

(41) Harlharan, P. C.; Pople, J. A. *Chem. Phys. Lett.* **1972**, *16*, 217.

(42) Davidson, E. R. In "The World of Quantum Chemistry"; Daudel, R., Pullman, B., Eds. D. Reidel Publishing, Co.: Dordrecht, 1974; p 17.

(43) Feller, D.; Davidson, E. R. *J. Chem. Phys.* **1981**, *74*, 3977.

the relative STO-3G energies are at least qualitatively correct. Thus, the following discussion focuses on the STO-3G results.

First, it should be noted that the TCSCF energy of 1A_1 , relative to the RHF energies of the other three TMM states, is anomalously low. As mentioned above and discussed in detail elsewhere,³⁷ this anomaly is due to the doublet instability problem. The problem is solved with an MCSCF or CI wave function, which provides electron correlation.

As observed previously by Dixon et. al.,²³ inclusion of electron correlation through use of an MCSCF wave function increases the energy difference between 1B_1 and 1B_2 from the RHF value. Our CI results confirm that this finding is not an artifact of their using a wave function with a limited number of configurations. We have previously discussed why such an increase should occur.^{18,25}

The same effect is observed with the SV basis set, although the increase on going to a correlated wave function is not as great with this more flexible basis set. Our SV-CI results also provide further evidence that 1B_1 is lower in energy than 1A_1 , although the energy difference is smaller than with STO-3G CI or STO-3G MCSCF.

As expected from Hammond's postulate, the energies of the transition states leading from MCP to 1B_1 and 1A_1 do, in fact, parallel the energies of these intermediates. There is also a small preference for a conrotary over a disrotary transition state connecting MCP with 1A_1 . Planar 1A_1 can also close to MCP by simultaneously pseudorotating and twisting one methylene group, giving 1B_1 as an intermediate along this reaction path. The barrier to this process is comparable in energy to those involving the simultaneous rotation of two methylene groups and to the barrier for pseudorotation²⁰ to an equivalent 1A_1 wave function.

The energy surface that we have calculated in the region around 1A_1 is sufficiently flat that dynamics could play an important role

in determining the partitioning of this intermediate. Our double Fourier series fit to the computed energy grid has provided a closed expression for the energy on the surface. Thus, trajectory calculations on the surface are feasible. These might provide some information regarding the molecular dynamics on the full 24-dimensional hypersurface, of which ours is but a two-dimensional projection.

Our Fourier fit to the singlet and triplet energies at the same set of geometries has enabled us to show that the lowest energy of intersection is actually above 1B_1 . Consequently, a surface intersection below the energy of 1B_1 cannot be invoked to reconcile the results of Dowd's EPR study with the calculated energy difference between $^3A'_2$ and 1B_1 . Tunnelling from one surface to another seems ruled out by Dowd's experiments.²⁸

It would now seem that there is little chance of reconciling Dowd's experimental results with the results of ab initio calculations. Either the best current approximations to the solution of the Schrödinger equation for 1B_1 and $^3A'_2$ are inadequate to give the energy difference between these states correctly, or Dowd's experiment does not measure the energy required for crossing from the triplet to the singlet surface. It should be noted, however, that the calculations refer to isolated TMM in the gas phase, whereas Dowd's experiments were done in frozen solutions. This difference remains the last hope for bringing theory and experiment into concordance.

Acknowledgment. We thank the National Science Foundation and the National Resource for Computation in Chemistry for supporting this work. Acknowledgement is also made to the donors of the Petroleum Research Fund, administered by the American Chemical Society, for partial support.

Registry No. MCP, 6142-73-0; TMM, 13001-05-3.

A New Method for Sequencing Fully Protected Oligonucleotides Using ^{252}Cf -Plasma Desorption Mass Spectrometry. 1. Negative Ions of Dinucleoside Monophosphates

Catherine J. McNeal,^{*,†} Kelvin K. Ogilvie,[†] Nicole Y. Theriault,[†] and Mona J. Nemer[†]

Contribution from the Departments of Chemistry, Texas A&M University, College Station, Texas 77843, and McGill University, Montreal, Quebec, Canada H3A 2K6.

Received May 18, 1981

Abstract: Using the method of californium-252 plasma desorption mass spectrometry we have established the systematics for a completely instrumental method of sequencing synthetic gene fragments which are in the intermediate stages of synthesis and therefore contain chemical protecting groups at all reactive sites. The fragmentation pattern for a variety of dinucleoside monophosphates has been identified and showed to contain ions which are diagnostic for the base sequence. The method is universally applicable to deoxy- and ribooligonucleotides containing a variety of different phosphate blocking groups.

A completely instrumental method for sequencing the chemically protected precursors of synthetic DNA and RNA has resulted from the synchronous developments in two independent fields of chemistry. The recent development of recombinant DNA techniques has stimulated the advancement of chemical procedures for synthesizing significant quantities of DNA and RNA. The synthetically assembled nucleic acids have been utilized in a multitude of novel experiments including the complete synthesis and cloning of biologically functional genes,¹ the study of the

regulator regions on a gene,² and exploration of the structure and function of nucleic acids.³ At the same time a new method in mass spectrometry, californium-252 plasma desorption mass spectrometry (^{252}Cf -PDMS),^{4,5} has evolved with capabilities that

(1) Wu, R.; Bahl, C. P.; Narang, S. A. *Prog. Nucleic Acids Res. Mol. Biol.* **1978**, *21*, 101-149.

(2) Itakura, K.; Riggs, A. D. *Science* **1980**, *209*, 1401-1405.

(3) Miller, P. S.; Braiterman, L. T.; Ts'o, P. O. P. *Biochemistry* **1977**, *16*, 1988-1996.

(4) Macfarlane, R. D.; Torgerson, D. F. *Science* **1976**, *191*, 920-925.

(5) Macfarlane, R. D.; Torgerson, D. F. *Int. J. Mass Spectrom. Ion Phys.* **1976**, *21*, 91-92.

[†] Texas A&M.

[†] McGill University.